

ANALOG MICROMIRROR ARRAYS WITH ORTHOGONAL SCANNING DIRECTIONS FOR WAVELENGTH-SELECTIVE $1 \times N^2$ SWITCHES

Jui-che Tsai, Sophia Huang, Dooyoung Hah*, and Ming C. Wu
 Electrical Engineering Department, University of California, Los Angeles
 Los Angeles, CA 90095-1594, U.S.A.
 TEL: 1-310-825-7338, FAX: 1-310-794-5513
 E-mail: jctsay@icssl.ucla.edu

* Microsystem Team, ETRI, 161 Gajeong-Dong, Yuseong-Gu, Daejeon, 305-350, South Korea

ABSTRACT

A new high-port-count wavelength selective switch has been realized using two cross-scanning 1-axis analog micromirror arrays in a 4- f optical system. The number of output ports is increased from N to N^2 , where N is the maximum linear port count limited by optical diffraction. Using surface-micromachined micromirrors with hidden vertical combdrives, large scan angles ($> \pm 5^\circ$ mechanical), low drive voltages (7V), and high fill factors ($> 96.25\%$) are achieved for both scanning mirrors. Experimental results of our 1×8 (3×3 collimator array) wavelength-selective switch are also reported. A fiber-to-fiber insertion loss of 6 dB and a switching time of $< 700 \mu\text{sec}$ have been achieved.

INTRODUCTION

Recent advances in wavelength-division-multiplexing (WDM) technologies have revolutionized the optical fiber communication networks. Wavelength-selective switches (WSS) have received a great deal of attention because their ability to route different wavelength channels independently. Joe Ford et al., proposed the first MEMS (Micro-Electro-Mechanical Systems)-based optical add/drop multiplexer (OADM) using a digital micromirror array [1]. The use of MEMS micromirrors offers lower insertion loss and faster speed than liquid-crystal-based OADM [2]. This OADM is essentially a 1×1 wavelength-selective switch. A multiport wavelength-selective switch can be realized by replacing the digital micromirrors with analog micromirrors and expanding the input/output fibers into a linear array. This is a useful network element because it can be used either as a versatile multiport add-drop multiplexer or as a basic building block for $N \times N$ wavelength-selective crossconnect (WSXC). Several $1 \times N$ WSS have been reported [3-9]. Table 1 summarizes the performances of published WSS's, including their port count, number of wavelength channels, channel spacing, and optical insertion loss. The maximum number of output ports reported to date is four, which is limited by optical diffraction. Larger port count (≥ 10) WSS is desired for high capacity networks.

In this paper, we report on a novel $1 \times N^2$ wavelength-selective switch by combining two one-dimensional (1D) arrays of 1-axis micromirrors with orthogonal rotation directions in a 4- f imaging system. This enables us to arrange the input/output fibers in a two-dimensional (2D)

array. The number of output ports is dramatically increased from N to N^2 . Experimentally, we have demonstrated a 1×8 WSS with a channel spacing of 75 GHz and an optical insertion loss of 6 dB. We have also performed theoretical modeling of the WSS, and shown that a 1×24 WSS can be realized in current optical configuration with optimized fiber collimator and mirror sizes.

Company/ Institution	port count	Number of wavelength channels	Channel spacing	Insertion loss
Lucent [4]	1x4	128	50 GHz	3 dB
Network Photonics [6]	1x4	96	50 GHz	-
Corning* [7]	2x2	80	50 GHz	< 7 dB
JDS Uniphase [8]	1x4	64	100 GHz	< 3.5 dB
UCLA [9]	1x4	30	200 GHz	5 dB
This paper	1x8	15**	75GHz	6 dB

*Liquid crystal switch

**Limited by the size of current MEMS chips.

Table 1. Comparison on wavelength-selective switches reported in the literature.

WAVELENGTH-SELECTIVE $1 \times N^2$ SWITCH

The schematic diagram of the $1 \times N^2$ wavelength-selective switch is shown in Figure 1. Two focusing lenses are arranged in a 4- f confocal configuration to image the first micromirror array in Plane A to the second micromirror array in Plane B. The grating is inserted between the lenses in the upper half of the system. The axial position of the grating is adjusted such that the projected light spot from the input port is located at the common focus of the two lenses. The 4- f configuration ensures that the optical beam focused on any mirror in the first array is always directed to the corresponding mirror in the second array, and vice versa, irrespective of the tilting angle of the mirrors. Thus each wavelength is steered by

two micromirrors in orthogonal directions and directed towards the desired output fiber in the 2D array.

Another benefit of this 4- f configuration is that the laser beam passes through the first array twice. This doubles the deflection of the laser beam in the vertical direction. Therefore, more spatial channels can be supported.

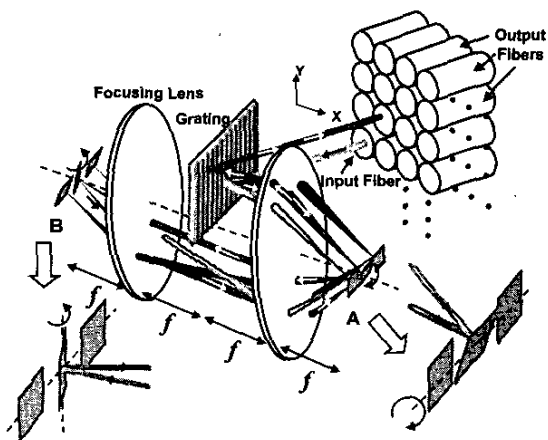


Fig. 1. Schematic setup of the $1 \times N^2$ wavelength-selective switch. The two orthogonally scanning micromirror arrays enable the fibers to be arranged in two dimensions, which increase the output port from N to N^2 .

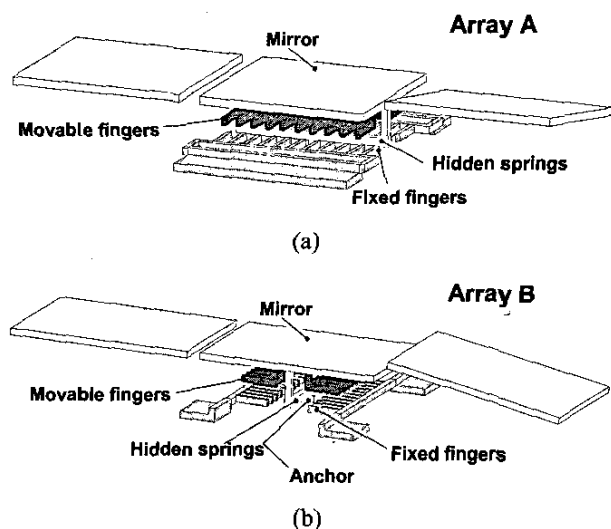


Fig. 2. Schematics of the analog micromirror arrays with hidden vertical comb-drive actuators. The scan directions of the mirrors are (a) perpendicular to, and (b) in parallel with the array directions.

ANALOG MICROMIRROR ARRAYS

Figure 2 shows the schematics of the analog micromirror arrays. The micromirrors that scan perpendicular to the array direction (Array A) have been reported in [3,5] and shown excellent stability in open-loop operations [9]. Similar vertical comb drives are employed in the micromirrors with orthogonal scan direction (Array B). The devices are fabricated using the SUMMiT-V surface-micromachining process provided by Sandia National

Laboratories [10]. It has five polysilicon layers, including one nonreleasable interconnect layer and four structural layers. The first two structural polysilicon layers are laminated to form lower combs. The third polysilicon layer is patterned into upper combs. The chemical-mechanical planarization (CMP) process before the deposition of the third polysilicon layer provides a clear separation between the upper and lower combs. The planar geometry also allows the finger spacing to be reduced to $0.5 \mu\text{m}$. The narrow gap spacing greatly increases the torque of the vertical comb actuators, which allows the mirror to operate at low voltages.

Figure 3 shows the scanning electron microscope (SEM) images of both micromirrors. The vertical combs and springs are completely covered by the mirrors. Furthermore, by eliminating the guiding structure between mirrors, high fill factors are achieved: 97.5% for Array A ($156 \mu\text{m}$ mirror on $160 \mu\text{m}$ pitch) and 96.25% for Array B ($154 \mu\text{m}$ mirror on $160 \mu\text{m}$ pitch). The design rules of SUMMiT-V permits fill factors as high as 99.4%. In these new devices, we have also extended the shielding electrode underneath the mirrors to increase the long-term stability [9]. Comb fingers near edges of the mirrors are removed to minimize crosstalk between adjacent mirrors caused by the fringe field.

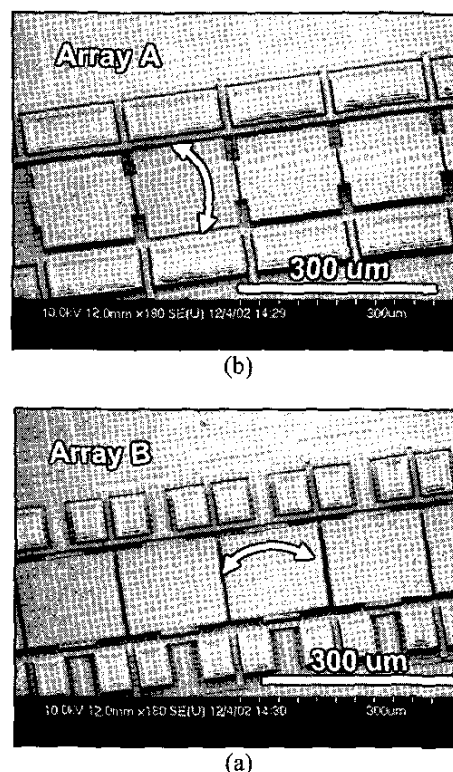


Fig. 3. SEM of micromirror arrays with (a) perpendicular and (b) parallel scan directions (in reference to the array direction).

The scan angles of the micromirrors are measured using a non-contact interferometric surface profiler (WYKO). Figure 4 shows the DC scan characteristics. The maximum mechanical scan angles are $\pm 5^\circ$ (7V) and $\pm 6.3^\circ$ (7.5V) for

arrays A and B, respectively. They are limited by lateral pull-in between the comb fingers.

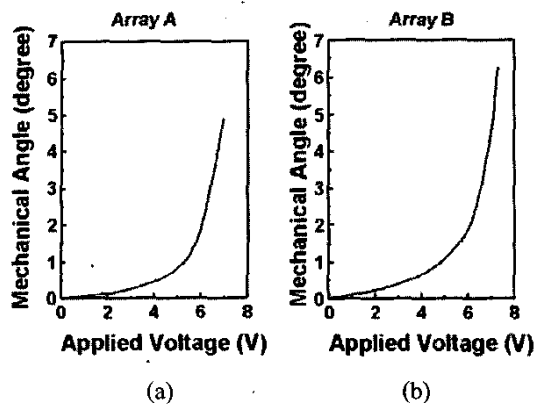
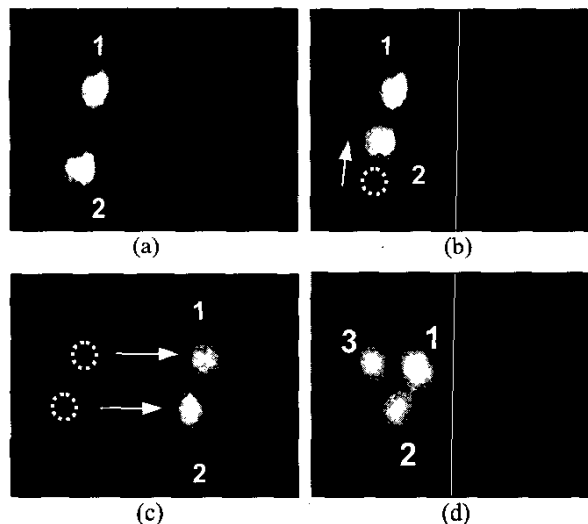


Fig. 4. DC scan characteristics of the micromirrors with (a) perpendicular and (b) parallel scan directions.

SYSTEM PERFORMANCE

Switching of different wavelength channels across the 2D plane is captured by an infrared camera and shown in Figure 5.



Bias Conditions	1550 nm		1552 nm	
	Vertical mirror(V1)	Horizontal mirror(V2)	Vertical mirror(V1)	Horizontal mirror(V2)
Fig. 5(a)	0	0	5.5 V	0
Fig. 5(b)	0	0	4.0 V	0
Fig. 5(c)	0	5.5 V	4.0 V	5.5 V

Fig. 5. Switching characteristics of the $1 \times N^2$ wavelength-selective switch. The wavelengths of channels 1, 2, and 3 are 1550, 1552, and 1550.8 nm, respectively.

Figure 5(a)-(b) show switching of the 1552-nm channel in the vertical direction, when the applied voltage on the corresponding vertical mirror changes from 5.5V to 4.0V. Figure 5(b)-(c) show switching of both 1550-nm and 1552-

nm channels in the horizontal direction. Figure 5(d) shows independent switching of 3 wavelengths to any arbitrary output channels. The table underneath list the bias conditions of each figure. The bias condition of Figure 5(d) is: $V_1 = 2.5V$, $V_2 = 0$ for the 1550-nm channel; $V_1 = 4V$, $V_2 = 0$ for the 1552-nm channel; $V_1 = 0$, $V_2 = 0$ for the 1550.8-nm channel.

We have constructed a prototype system using lenses with 15-cm focal lengths. A channel spacing of 75 GHz is attained with an 1100 grooves/mm grating. The number of wavelength channels is 15, which is limited by the number of mirrors in the array that can be accommodated on the SUMMIT-V chip. The optical system supports a 3×3 fiber collimator array at the input plane, which can be used as a 1×8 wavelength-selective switch with input collimator located at the center of the array. Currently, discrete collimators are used to simulate the 2D array. The focused beam waist on the micromirror is 30 μm . With the micromirror pitch of 160 μm , the acceptable beam waist can be as large 60 μm [11]. Using this number, the input collimator size can be reduced by two times. Hence, the array size at the input plane can be increased to 5×5 , which can be used for a 1×24 wavelength-selective switch.

The fiber-to-fiber insertion loss of the system is measured to be 6 dB when the laser beam is coupled back to the input fiber collimator. Figure 6 shows the temporal response when a square wave is applied to both arrays. The switching time is 150 μsec at the falling edge, and 700 μsec at the rising edge. The extinction ratio is 35 dB.

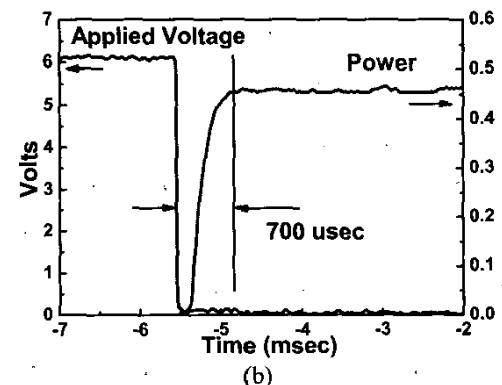
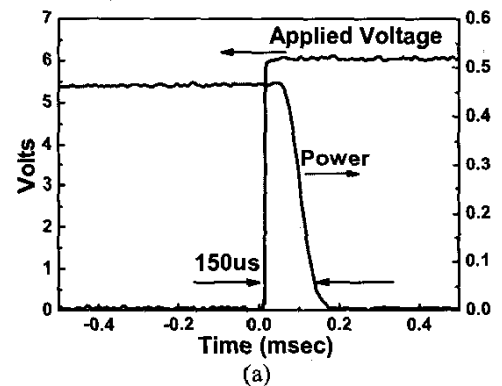


Fig. 6. Measured switching time of the wavelength-selective $1 \times N^2$ switch: (a) falling edge, (b) rising edge.

When the laser beam is switched to a fiber channel right below the input collimator, the insertion loss is measured to be 8.6 dB. When switched to a diagonal channel at one of the corners, the insertion is 14 dB. The difference in insertion loss is attributed to the imperfect optical alignment. Figure 7 shows the spectral response at the input and the diagonal output fibers. Ten of the fifteen wavelength channels are shown in the plots. Switching at 1550 nm is clearly observed. The ripples at 1552.5 nm are due to a broken mirror in array, which scatters light into to the output channel.

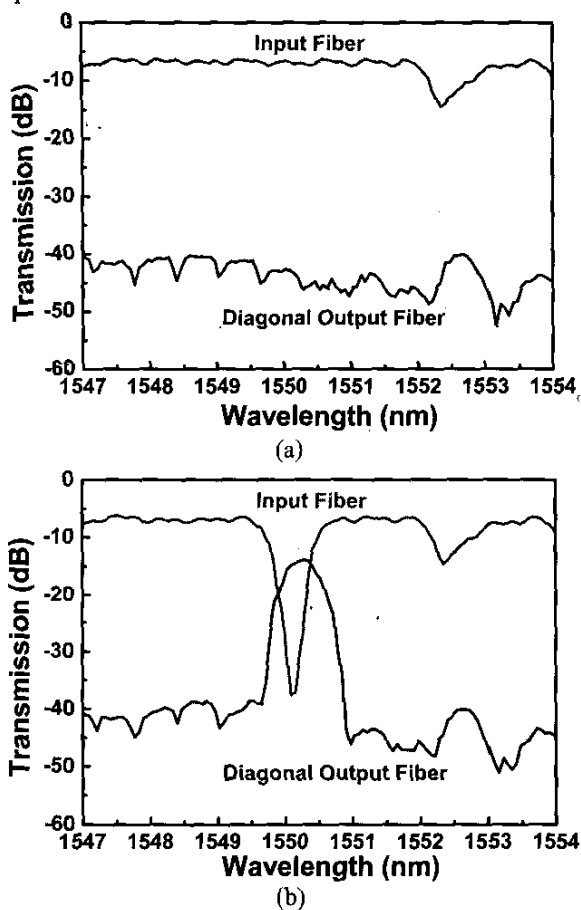


Fig. 7. Spectral response at the input and output fibers, when (a) all the wavelength channels are coupled back to the input fiber, (b) the signal of 1550 nm is switched to the output fiber in the diagonal direction. The ripples around 1552.5 nm are due to a broken mirror.

CONCLUSION

We have successfully demonstrated a $1 \times N^2$ wavelength-selective switch using two cross-scanning 1-axis micromirror arrays in a confocal geometry. Using surface-micromachined micromirrors with hidden vertical combdrives, large scan angles ($> \pm 5^\circ$ mechanical), low drive voltages (7V), and high fill factors ($> 96.25\%$) are achieved for both scanning mirrors. By arranging the input/output fibers in a two-dimensional array, the number of output

ports is dramatically increased from N to N^2 . The 1×8 prototype WSS with 75 GHz channel spacing exhibited a fiber-to-fiber optical insertion loss of 6 dB, a switching time less than 700 μ sec, and an extinction ratio of 35 dB. By further optimizing the mirror and the collimator sizes, the port count of the current optical system can be expanded to 1×24 .

ACKNOWLEDGEMENT

This project is supported by DARPA/SPAWAR under contract N66001-00-C-8088. The authors would like to thank Professor Joe Ford at University of California, San Diego for helpful discussions, and Ming-Chang Lee and Josh Chi of UCLA for SEM images and technical assistance.

REFERENCE

- [1] J. E. Ford, V. A. Aksyuk, D. J. Bishop, and J. A. Walker, "Wavelength add-drop switching using tilting micromirrors," *J. Lightwave Technology*, vol.17, p.904-11, 1999.
- [2] J. S. Patel and Y. Silberberg, "Liquid crystal and grating-based multiple-wavelength cross-connect switch," *IEEE Photon. Technol. Lett.*, 7, 514-516 (1995).
- [3] D. Hah, S. Huang, H. Nguyen, H. Chang, H. Toshiyoshi, and M. C. Wu, "A low voltage, large scan angle MEMS micromirror array with hidden vertical comb-drive actuators for WDM routers," *OFC 2002*, TuO3.
- [4] D. M. Marom, et al., "Wavelength-selective 1×4 switch for 128 WDM channels at 50GHz spacing," *2002 OFC postdeadline paper*, FB7.
- [5] D. Hah, S. Huang, H. Nguyen, H. Chang, J. C. Tsai, and M. C. Wu, "Low voltage MEMS analog micromirror arrays with hidden vertical comb-drive actuators," *Solid-State Sensor, Actuator, and Microsystems Workshop*, June 2002, p.11-14.
- [6] <http://www.networkphotonics.com>
- [7] A. R. Ranalli, B. A. Scott, J. P. Kondis, "Liquid crystal-based wavelength selectable cross-connect," *ECOC 1999*.
- [8] T. Ducellier, et al., "The MWS 1×4 : a high performance wavelength switching building block," *ECOC 2002*.
- [9] S. Huang, J. C. Tsai, D. Hah, H. Toshiyoshi, and M. C. Wu, "Open-loop operation of MEMS WDM routers with analog micromirror array," *2002 IEEE/LEOS Optical MEMS Conf.*
- [10] <http://www.sandia.gov/mstc/technologies/micromachines/summit5.html>
- [11] D. M. Marom, and Sang-Hyun Oh, "Filter-shape dependence on attenuation mechanism in channelized dynamic spectral equalizers," *LEOS 2002*.